

# Relationship between Forbush Effect Parameters and the Heliolongitude of Solar Sources

M. A. Abunina, A. A. Abunin, A. V. Belov, E. A. Eroshenko, A. S. Asipenka,  
V. A. Oleneva, and V. G. Yanke

*Pushkov Institute of Terrestrial Magnetism, Ionosphere, and Radiowave Propagation, Russian Academy of Sciences  
(IZMIRAN), Troitsk, Moscow, 142190 Russia*

*e-mail: abunina@izmiran.ru*

Received September 13, 2011

**Abstract**—All significant events in galactic cosmic rays for the last 55 years have been collected in a Forbush effect database created at the Pushkov Institute of Terrestrial Magnetism, Ionosphere, and Radiowave Propagation (hereinafter, IZMIRAN) based on data from the global network of neutron monitors. The solar sources of ~800 of these events have been identified. These events were divided into five groups with respect to the heliolongitudes of the associated X-ray solar flares, and typical behavior of their characteristics such as cosmic ray density and anisotropy, was studied independently for each group. The Forbush effect characteristics, which are the most dependent on the source heliolongitude, have been identified.

**DOI:** 10.1134/S0016793213010027

## 1. INTRODUCTION

The largest Forbush effects (FEs) are directly caused by propagating solar wind disturbances generated by coronal mass ejections (CMEs) (Iucci et al., 1979; Richardson and Cane, 1993; Cane et al., 1994). The beginning of such an FE coincides with the arrival of an interplanetary shock and geomagnetic storm sudden commencement (SSC). A possible correlation between some FE parameters and CME characteristics and solar sources (specifically, heliolongitudinal dependence of FEs) has been considered in many works (Sino, 1961; Haurvitz et al., 1965; Barnden, 1973; Iucci et al., 1985, 1986; Cane, 1996, 2000; Belov et al., 2001). The first detailed study was performed in (Iucci et al., 1985, 1986). However, a huge amount of new data on events on the Sun and in the interplanetary medium has been accumulated since then, which gives new possibilities for studies. A statistical analysis of such events requires a large data volume since, as was noted in (Cane, 2000), the situation in the Earth's orbit can be very complex owing to interaction of several transient events that are close in time and space (see also (Burlaga et al., 2003; Gopalswamy et al., 2004)). It is difficult to separate FEs caused by different types of disturbances (Crooker and Cliver, 1994; Gonzalez et al., 1996; Cliver and Cane, 1996; Belov, 2009).

In addition, almost all of the above works analyzed FEs for relatively short periods of time and insignificant numbers of events, mainly, based on data of one to three individual neutron monitors (NMs). The difference in variations in NM count rates between different stations during FEs depends on the properties of

each station, as a result of which it is impossible to exactly characterize an event. Since the geographic position, altitude, and geomagnetic cutoff rigidities can be different, a Forbush decrease (FD) can show different depths, time profiles, and even onset times in the count rate at each station. Therefore, it is better to use FE characteristics which are independent on the observation site in an analysis: the density and anisotropy of cosmic rays (CRs) obtained using the global survey method based on world wide NM network data (Belov et al., 2005a).

In this work, we only study nonrecurrent FEs: events related to CMEs and associated with solar sporadic sources. The aim of the work is to reveal the tendencies in the CR anisotropic behavior which manifest themselves in the dependence of anisotropy on the FD value, delay of the FE onset relative to the disturbance arriving, and the CR intensity decrease rate during the main FD phase for FEs distributed by different heliolongitudinal groups of their sources. Similar studies use CRs as an information source of a different type: these studies give additional possibilities for localizing an interplanetary disturbance solar source, make it possible to understand how disturbances propagate from different sources and when and why they become geoeffective, and feed us with additional information in order to estimate the structure and dimensions of interplanetary disturbances caused by different sources.

## 2. DATA AND METHODS

Two databases developed at IZMIRAN were used to study the relations between solar flares and FEs near the

Averaged parameters for all FEs with identified solar sources within different heliolongitudinal sectors from 1976 to 2010

	E91–E46	E45–E16	E15–W15	W16–W45	W46–W91
$A_F$	$2.47 \pm 0.28$	$2.90 \pm 0.23$	$3.00 \pm 0.30$	$2.95 \pm 0.39$	$2.26 \pm 0.26$
$A_{xy_{\max}}$	$1.58 \pm 0.08$	$1.75 \pm 0.07$	$1.81 \pm 0.09$	$2.15 \pm 0.17$	$2.01 \pm 0.16$
$A_{z_{\text{range}}}$	$1.72 \pm 0.11$	$1.94 \pm 0.08$	$1.98 \pm 0.09$	$2.04 \pm 0.11$	$1.92 \pm 0.16$
$D_{\min}$	$-0.56 \pm 0.07$	$-0.57 \pm 0.04$	$-0.66 \pm 0.06$	$-0.81 \pm 0.12$	$-0.60 \pm 0.10$
$D_{\max}$	$0.80 \pm 0.36$	$0.37 \pm 0.02$	$0.49 \pm 0.08$	$0.49 \pm 0.05$	$0.39 \pm 0.02$
$Kp_{\max}$	$5.00 \pm 0.21$	$5.24 \pm 0.17$	$5.73 \pm 0.15$	$5.79 \pm 0.19$	$5.41 \pm 0.21$
$Ap_{\max}$	$59.13 \pm 6.02$	$67.21 \pm 6.52$	$88.43 \pm 6.35$	$92.12 \pm 8.56$	$75.70 \pm 9.80$
$Dst_{\min}$	$-58.0 \pm 5.8$	$-72.0 \pm 6.9$	$-85.5 \pm 5.9$	$-87.9 \pm 8.5$	$-67.2 \pm 6.8$
$B_{\max}$	$15.03 \pm 0.89$	$17.68 \pm 1.13$	$17.91 \pm 0.75$	$17.47 \pm 1.39$	$18.21 \pm 1.33$
$V_{\max}$	$521.7 \pm 19.2$	$569.4 \pm 14.8$	$541.1 \pm 13.6$	$564.0 \pm 18.0$	$597.3 \pm 21.2$
$V_m B_m$	$4.04 \pm 0.31$	$5.13 \pm 0.45$	$5.07 \pm 0.31$	$5.13 \pm 0.56$	$5.52 \pm 0.55$
$t_{\min}$	$24.75 \pm 2.64$	$22.12 \pm 1.71$	$18.06 \pm 1.53$	$13.48 \pm 1.94$	$16.02 \pm 2.55$
$t(D_{\min})$	$12.68 \pm 2.22$	$11.99 \pm 1.51$	$11.16 \pm 1.22$	$9.16 \pm 1.67$	$11.57 \pm 1.93$
$A_F/B$	$0.166 \pm 0.021$	$0.163 \pm 0.012$	$0.156 \pm 0.013$	$0.149 \pm 0.013$	$0.132 \pm 0.014$
$H_{\text{Lon}}$	$-66.725 \pm 1.997$	$-29.963 \pm 0.912$	$0.253 \pm 0.882$	$28.507 \pm 1.042$	$63.915 \pm 2.000$

Note: The sources are distributed over five longitudinal groups and are spaced by 48 before and 48 h after one another, respectively (344 events).

Earth. The first database (Belov et al., 2005b) contains information on all X-ray flares registered by the GOES satellites ([ftp://ftp.ngdc.noaa.gov/STP/SOLAR\\_DATA/SOLAR\\_FLARES/XRAY\\_FLARES/](ftp://ftp.ngdc.noaa.gov/STP/SOLAR_DATA/SOLAR_FLARES/XRAY_FLARES/)) from autumn 1975 to the present. The second database (Belov, 2009) includes the characteristics of FEs and interplanetary disturbances. The parameters of each FE (hourly values of density and CR anisotropy outside the magnetosphere) were calculated based on the NM network data using the global survey method (GSM) (Belov et al., 2005a). These parameters are global characteristics independent of individual detectors. Our database uses data for CRs with a rigidity of 10 GV since this rigidity is close to the effective rigidity of particles registered with NMs. The maximal FD values, FD onset time, time of reaching an FE minimum, and the duration of the main FE phase were estimated for each event and introduced into the database. The maximal IMF and solar wind (SW) values, as well as the times of these maximums relative to the shock arrival, were calculated from the OMNI database (<http://omniweb.gsfc.nasa.gov/ow.html>). The IZMIRAN database also includes the maximal values of the CR anisotropy components and the  $Kp$  and  $Ap$  geomagnetic activity indices (<ftp://ftp.gfz-potsdam.de/pub/home/obs/kp-ap/wdc/>) for each event.

For analysis, we selected FEs:

- (1) identified with solar sources;
- (2) separated by a time interval of at least 48 h from one another in order to avoid the superposition of

multiple events or (when the interval is shorter) when the value of the previous FD is  $<1.5\%$ .

Our database included 334 such events during the period from 1976 to 2010. They were divided into five groups with respect to the heliolongitudinal ranges of their solar sources: E91–E46, E45–E16, E15–W15, W16–W45, and W46–W91. The series of parameters, some of which (used in the analysis) are presented in the table, was determined and introduced for each group.

To obtain this table and other results discussed below, we used the properties and possibilities of the database that make it possible to select events with respect to different parameters and make different correlation and statistical estimations.

### 3. DISCUSSION OF RESULTS

The FE parameters for each longitudinal group of solar sources and the characteristics of the interplanetary medium and solar wind state during the considered periods are presented in the table. Here  $A_F$  is the averaged of FD maximum value;  $A_{xy_{\max}}$  is the maximal value of the equatorial component of the first CR anisotropy harmonic;  $A_{z_{\text{range}}}$  is the range of variations in the anisotropy north–south component;  $D_{\min}$  is the maximal decrease in the CR density per hour;  $D_{\max}$  is the maximal increase in the CR density;  $Kp_{\max}$ ,  $Ap_{\max}$ , and  $Dst_{\min}$  are the maximal values of the geomagnetic activity indices during the considered events;  $B_{\max}$  is the maximal IMF intensity;  $V_{\max}$  is the maximal SW

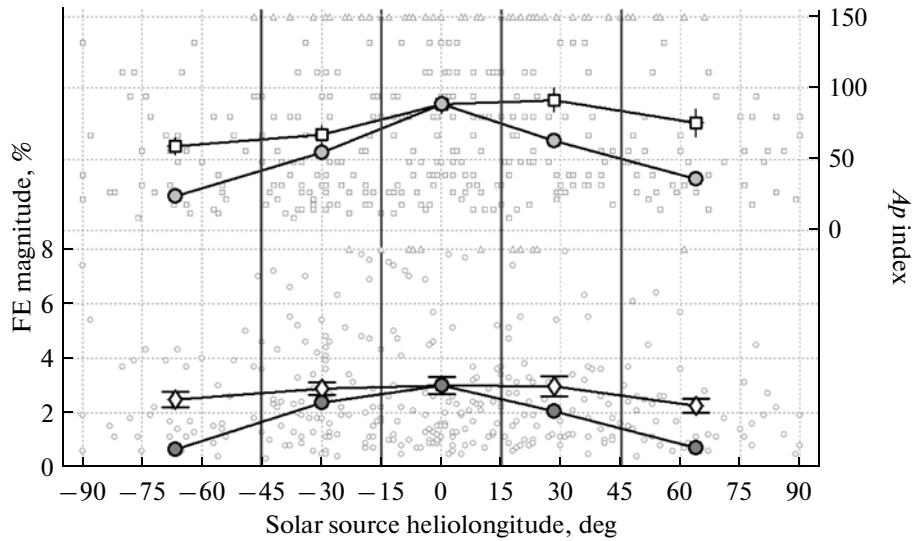


**Fig. 1.** Dependence of the FD and geomagnetic activity  $A_p$  indices on the solar source longitude. The largest events with FD  $> 8\%$  and with an increase in the  $A_p$  index larger than 150 (2 nT) are marked with triangles at the top of the figure ( $\square$  and  $\diamond$ —observable results;  $\circ$ —calculated with accounting of the full number of events).

velocity; and  $V_m B_m$  is the product of the maximal characteristics of the interplanetary medium in the considered disturbance calculated from the formula

$$V_m B_m = \frac{V_{\max}}{V_0} \frac{B_{\max}}{B_0}, \quad (1)$$

where  $V_0$  and  $B_0$  are the parameters of a quiet medium ( $V_0 = 400$  km/s and  $B_0 = 5$  nT are used as a rule);  $t_{\min}$  is the time from the onset to the density minimum in an FD;  $t(D_{\min})$  is the time of the maximal hourly density decrease during the main FD phase;  $A_f/B_{\max}$  is the ratio of the FD amplitude to the maximal IMF intensity; and  $H_{\text{Lon}}$  is the source heliointitude.

Among the events selected using the method described above, 99 effects were caused by the solar disk central sector (E15–W15); 81 events, by the near eastern sector (E45–E16); 67 events, by the near western sector (W16–W45); and 40 and 47 events, by the far eastern (E91–E46) and western (W46–W91) sectors, respectively (Fig. 1).

We should take into consideration that almost all disturbances get to the Earth from the central zone and only some disturbances come from other zones; in this case, the weakest ejections are filtered out. Only the largest and most powerful ICMEs come from distant longitudes. In the far eastern and western sectors, the values of the observed FDs are also slightly increased.

It is natural to assume that the number of ejections per each degree of longitude from the eastern sector was the same as such a number of ejections from the central zone; however, these ejections mostly passed east of the Earth and did not affect CRs that reached the Earth. Therefore, these ejections were not included in our database. Roughly speaking, only one

of three eastern ejections affects the SW and CRs near the Earth. Taking into account only these events, we obtain a substantially increased effectiveness of ejections from sources located at large distances along heliointitude. If we wanted to calculate the average effect caused by an eastern ejection, we would add  $99 \times 1.5 - 40 = 109$  zero events to 40 observed FDs (we also make corrections for the fact that this sector is larger along longitude by a factor of 1.5). For the near-eastern sector, we add  $99 - 81 = 18$  zero events, respectively.

In such a case, the average effect would be  $40 \times 2.47 / (99 \times 1.5) = 0.67$ ,  $47 \times 2.26 / (99 \times 1.5) = 0.72$ ,  $81 \times 2.90 / 99 = 2.37$ , and  $67 \times 2.95 / 99 = 1.99\%$  for the eastern, western, near-eastern, and near-western sectors, respectively. This effect would remain unchanged (3.00%) in the central sector (Fig. 1).

Thus, the actual difference in the FD value between the central and eastern and western sectors would be by factors of  $\sim 4.5$  and 4.2 rather than several tens of percentage points, respectively.

To all appearance, the statistics of eastern ejections generating FEs mainly depend on the distribution of their longitudinal dimension. This statistic indicates that such ejections are mostly no larger than  $45^\circ$  in half-width.

The situation is slightly different concerning western ejections. Owing to the IMF geometry, we sometimes can observe variations in CRs from a far western source, even when ICME generating these rays passes far from the Earth. Thus, the FD region is (in its eastern zone) wider than the ejection region or the region occupied by an interplanetary disturbance. However, we have not to forget that the FD value in this eastern zone is smaller than in the western zone owing to the

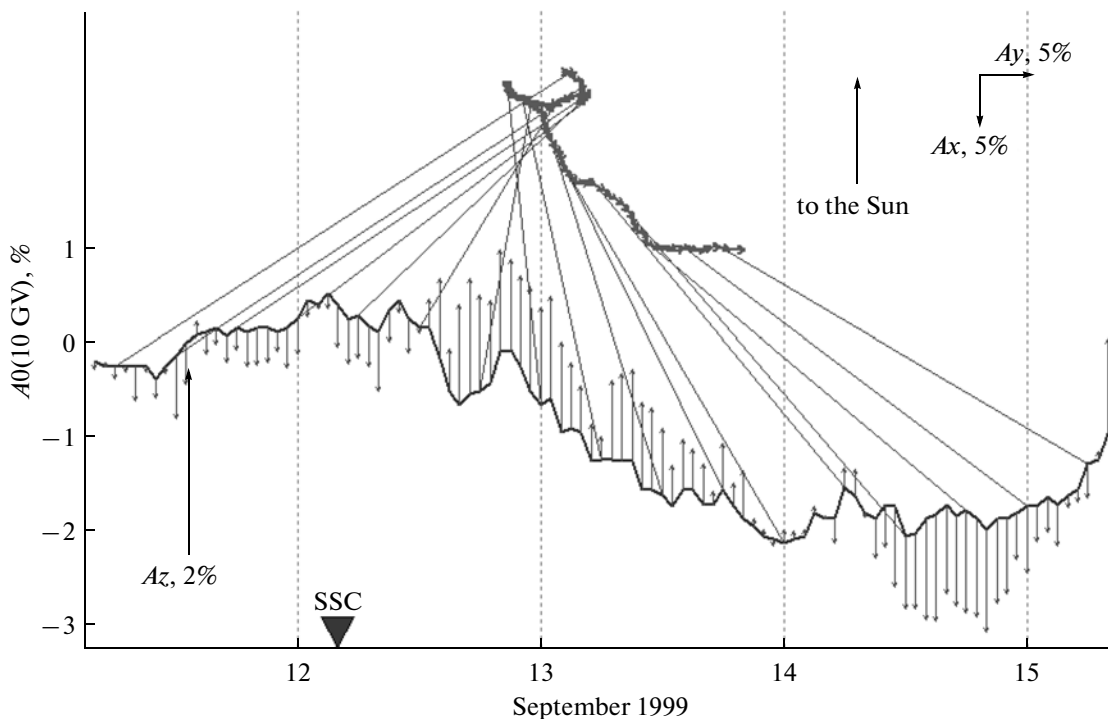


**Fig. 2.** Behavior of the CR density and vector anisotropy during an FE caused by a far eastern source (the heliologitude of an associated flare is E53).

same geometry. Therefore, the number of FDs in the western sector is apparently larger than in the eastern one, but their average value is much smaller.

Each group includes various events, but we nevertheless tried to distinguish the most typical events among them. Examples of such events are presented in Figs. 2–6. A solid curve in each figure corresponds to the profile of the isotropic part of variations (density) in CRs with a rigidity of 10 GV, and the vector diagram presents hourly values of the CR anisotropy equatorial component vector. The vertical vectors show a change in the north–south CR anisotropy component, and the thin lines join identical instants on the vector diagram and the CR density curve at an interval of 6 h.

Forbush effects caused by far eastern sources are characterized by small values (mainly 2–3%; the total spread varies from 0.4 to 7%), an extensive decline phase (a minimum can be reached one to three days later), and a low decrease rate during the decline phase. During these events, the CR anisotropy is as a rule insignificant (the equatorial component of the first harmonic), but variable, in direction, especially during the decline phase, up to a complete vector rotation (see Fig. 2).

Figure 3 presents an example of a typical FE caused by an eastern source with a heliologitude of E37, located at a smaller distance from the center. These events differ from the previous group by a larger effect value (mainly 3–4%, although the spread in values varies from 0.3 to 20%). An FD minimum is reached

in a shorter period of time (about a day), but, as before, the recovery process is slow. In these cases, the anisotropy behavior remains very complex and the equatorial component vector rotates during the entire FE.

The events related to the central group of sources (see Fig. 4) are characterized by a large FD amplitude (as a rule, 3% and more; the spread in values is 0.3–20%), short  $t_{\min}$  (a minimum is often reached in several hours), and, consequently, considerable decrement  $D_{\min}$ . The anisotropy behavior becomes simpler, and its direction becomes more stable (from east to west), although certain changes in direction are still pronounced during the main decrease phase. In addition, anisotropy sharply increases during the main FD phase.

Sources from relatively low western heliologitudes (Fig. 5) as a rule give small FEs when a minimum is reached rapidly. A high level of anisotropy and its stable direction from east to west are achieved because the disturbed region is open from the eastern side.

Forbush decreases caused by far-western sources are usually insignificant (not more than 2%), rapid, and short-lived (Fig. 6). However, the anisotropy level is often very high and stable in direction during long periods of time throughout these events. It is high even when an FD almost ended and the CR recovered its level. It seems that the Earth is for a long time affected by a disturbed region through CR anisotropy, being out of this region.

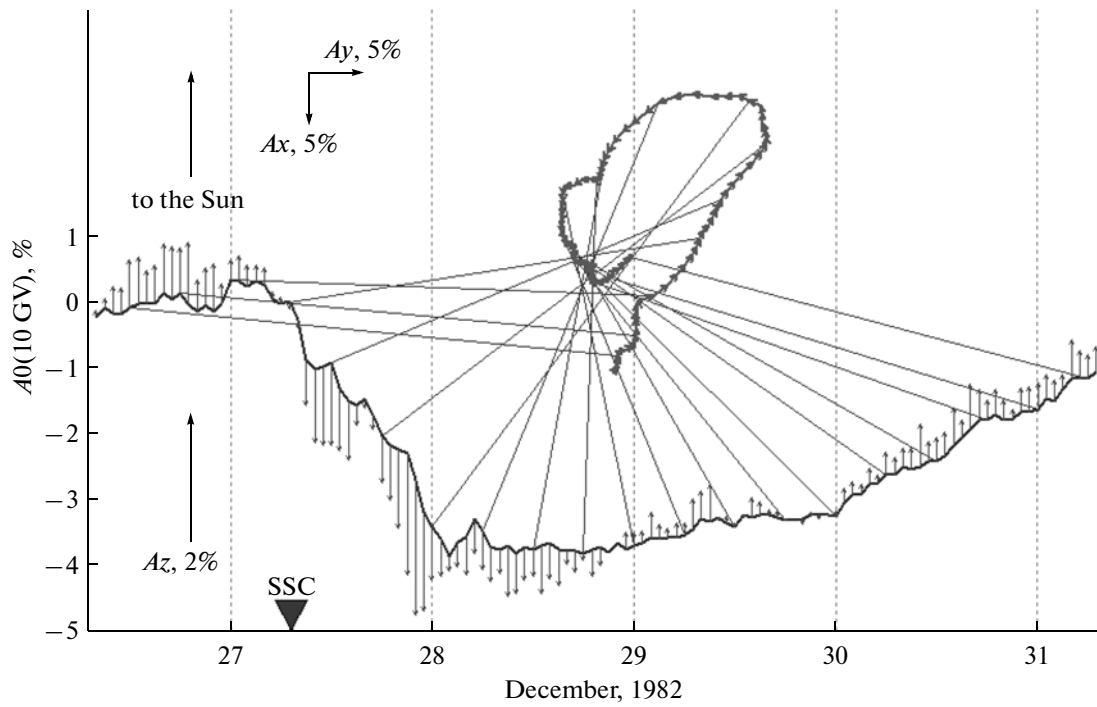


Fig. 3. Behavior of the CR density and vector (daily) anisotropy during FEs caused by a eastern source (E37).

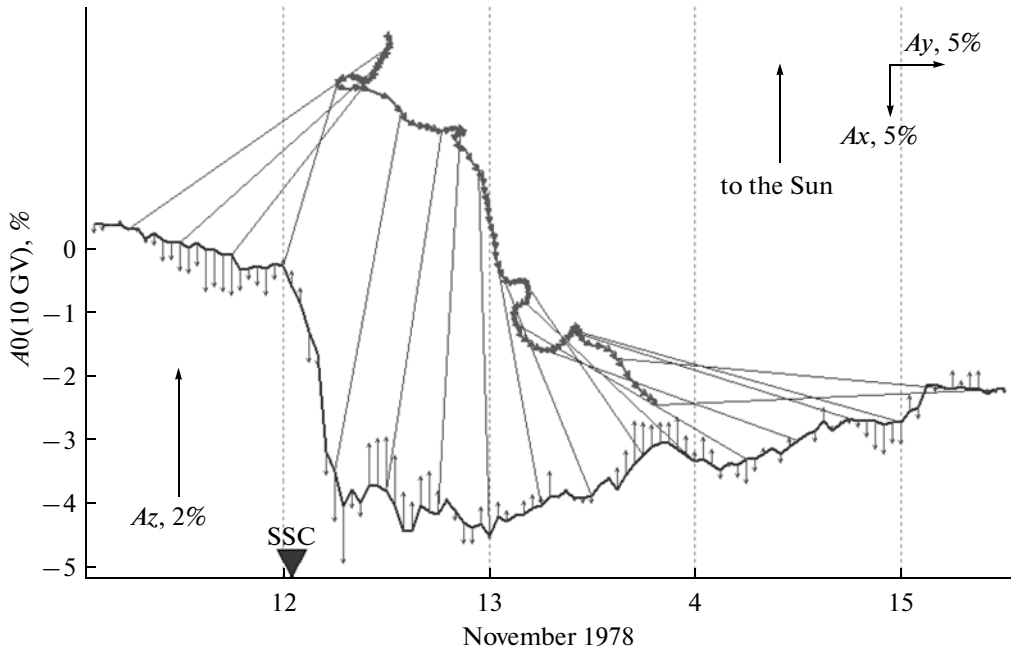


Fig. 4. Behavior of the CR density and daily anisotropy vector during FEs caused by sources from the region of central heli-longitudes (E02).

Figures 2–6 indicate that the behavior of the CR vector anisotropy differs considerably in different source longitudinal sectors. For eastern and central events, the behavior is the most complex and is accompanied by the rotation of the equatorial component vectors. For FEs caused by western sources,

anisotropy increases and becomes more stable in direction.

For different groups, we obtained parameters characterizing the relation between the CR anisotropy equatorial component and the FD amplitude  $((A_{xy_{max}} - A_{xy_q})/A_F)$ .

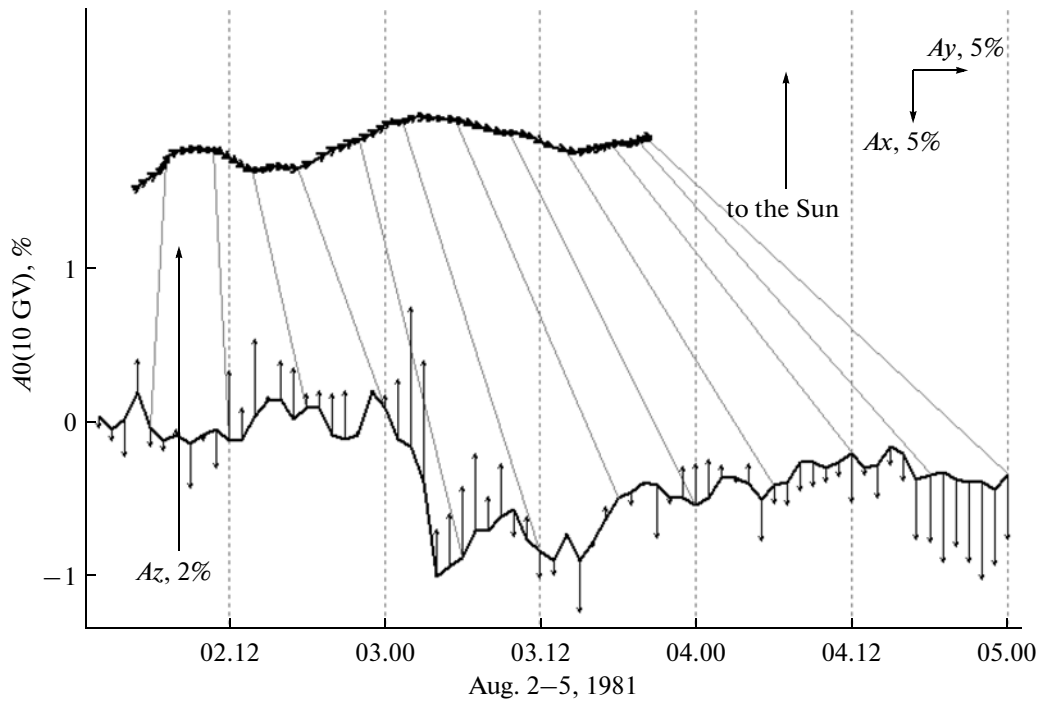


Fig. 5. Behavior of the CR density and vector anisotropy during an FE caused by a source from the western group (W20).

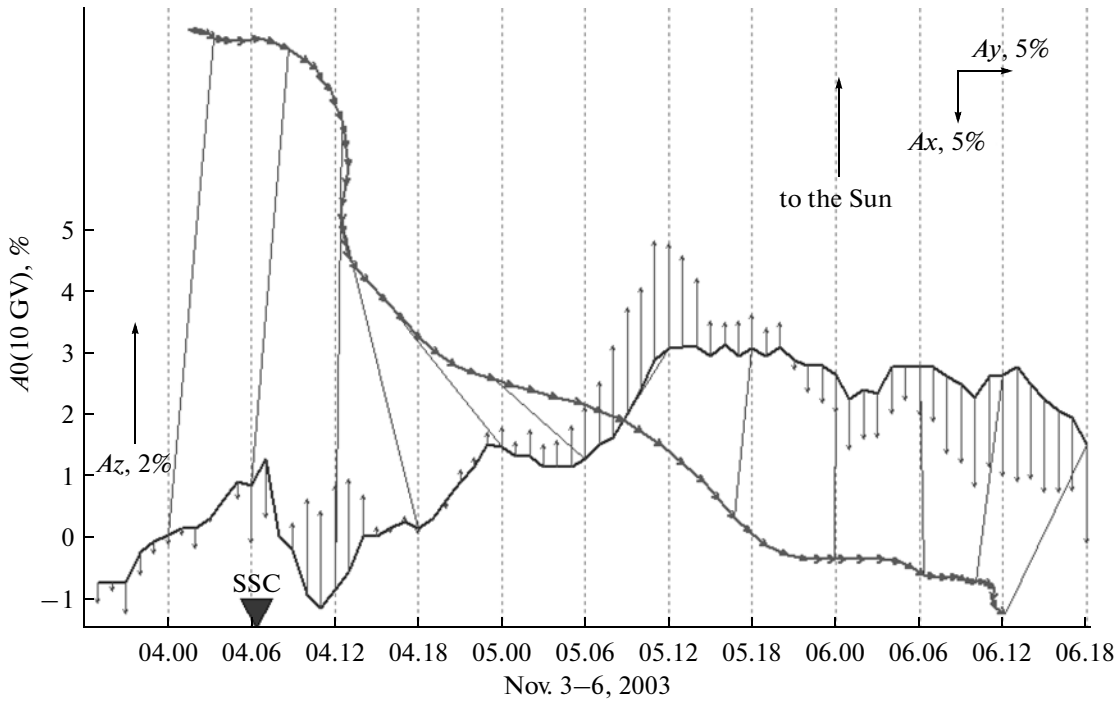
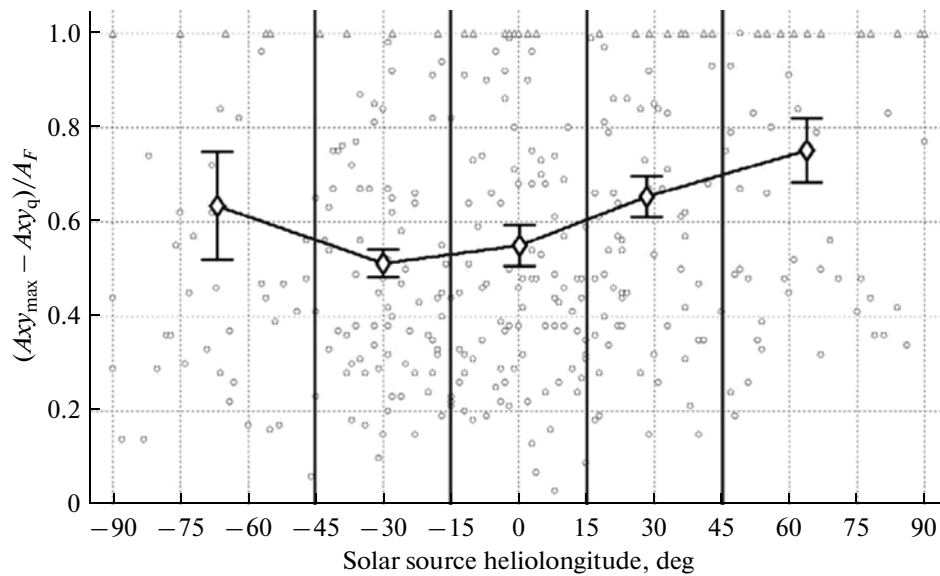


Fig. 6. Behavior of the CR density and vector anisotropy during an FE caused by a far western source (W56).

where  $A_{xy_q}$  is the average annual  $A_{xy}$  value during quiet periods), as well as the times of reaching the FD minimum ( $t_{min}$ ) and the maximal CR intensity decrease rate ( $t(D_{min})$ ). Variations in these parameters

vs. the solar source heliolongitude are presented in Figs. 7 and 8.

We also obtained parameter  $A_F/B_{max}$ , which characterizes the relation between the FD amplitude and



**Fig. 7.** Relation between  $A_{xy}$  and the FD amplitude ( $A_F$ ) depending on the source heliolongitude.

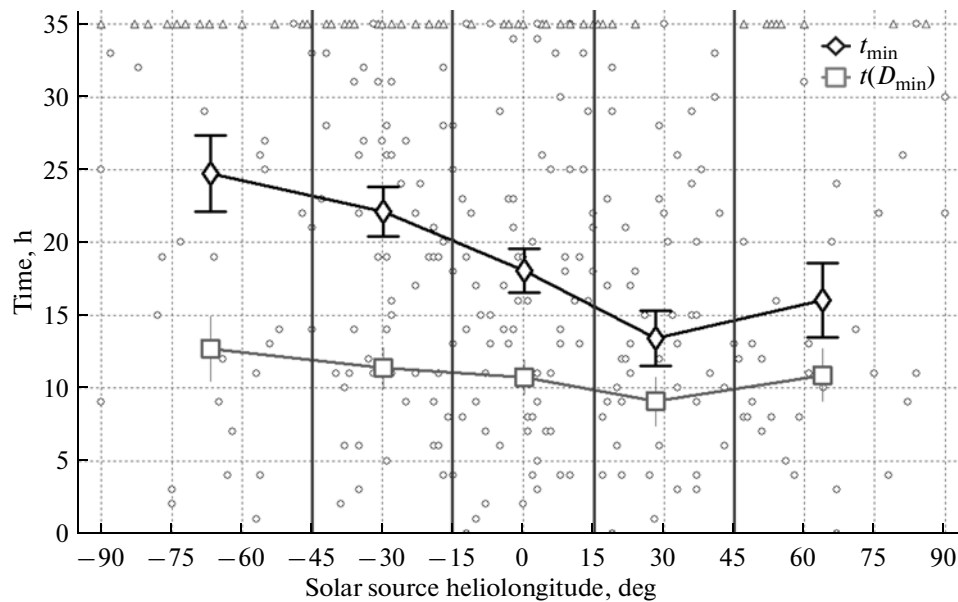


**Fig. 8.** Variations in the time of reaching an FD minimum ( $t_{\min}$ ) and in the time of the maximal decrement during the FE decline phase ( $t_{D_{\min}}$ ).

the IMF value. The analysis of the behavior of this parameter showed that the FD value ( $A_F$ ) per unit IMF intensity ( $B_{\max}$ ) is larger for eastern events than for western ones, which means that the effectiveness of eastern sources in the generation of FEs is slightly higher (Belov et al., 2009). During the events caused by eastern sources, the Earth is in the western peripheral zone of an SW disturbance. This disturbance zone is closed for the CR exchange (in contrast to events

with western sources), and an FD should be rather large and prolonged here.

Figure 7 presents the behavior of the parameter  $(A_{xy_{\max}} - A_{xy_q})/A_F$  depending on the source heliolongitude.  $A_{xy_q}$  (anisotropy during quiet periods) should be taken into consideration because CR anisotropy is perennial (its average value for 10 GV is  $\sim 0.5\%$ ) and is (as a rule) increased by interplanetary disturbances. It is clear that the relation between the CR anisotropy

and the FD amplitude increases with increasing distance of a source westward from the solar center. The anisotropy becomes very high (sometimes even larger than density variations) in FEs caused by far western sources. Since a disturbed region is open from the eastern side, recovery is rapid and a particle flux directed from east to west can be observed.

The considered dependences can be a source of additional information for space weather forecasts. For example, if small  $A_F/B_{\max}$  and relatively large  $A_{xy_{\max}}/A_F$  values are observed, the FE source is probably western. Thus, we obtain additional factors that make it possible to estimate the source longitude and often separate western events caused by eastern and central ones.

The characteristics presented in Fig. 8 indicate how an event developed. For example, the faster evolution of the effect from the western source, the smaller and shorter it is: a decrease has no time to develop completely since the Earth leaves a disturbed region rapidly. Eastern events develop slower since a disturbed region as if flows around the Earth. The development of events caused by far eastern sources is the slowest, and that of effects caused by moderately western sources is the fastest.

Sometimes, when a western source is very distant, the Earth can be outside the disturbed region and we will not observe a decrease in the CR density. However, variations in CR anisotropy (specifically, a substantial increase in anisotropy) will be considerable for a long period of time, and the Earth can “observe” this source from a distance in CRs.

#### 4. MAIN CONCLUSIONS

A comparison of FEs caused by sporadic solar sources (CMEs) from different solar disk zones indicates that different FE parameters depend substantially on the source heliolongitude.

The direction of the CR anisotropy during FEs is more variable for eastern and central sources and is more stable for western ones.

Effects associated with eastern CMEs develop most slowly.

The FE anisotropy and the ratio of the observed anisotropy to the CR density variations in this FE increase with decreasing distance of a source to the solar disk western edge.

The group of FEs with moderately western sources is characterized by rapid development (specifically, by the rapid formation of an FD minimum).

Further analysis will also make it possible to reveal other FE parameters substantially dependent on the source heliolongitude. The knowledge of such dependences gives additional information regarding the causes of SW disturbances, makes it possible to predict the further development of these disturbances, and is of prognostic importance.

#### ACKNOWLEDGMENTS

We are grateful to the personnel of the cosmic ray stations that provide data on the continuous registration of the neutron component (<http://cr0.izmiran.ru/> ThankYou).

This work was partially supported by the Russian Foundation for Basic Research (project no. 11-02-01478), Presidium of the Russian Academy of Sciences (Program no. 6 “Neutrino Physics”), and the Ministry of Science (state contract no. 14.740.11.0609).

#### REFERENCES

- Barnden, L.R., Forbush Decreases 1966–1972; Their Solar and Interplanetary Associations and Their Anisotropies, *Proc. 13th ICRC*, Denver, 1973, vol. 2, pp. 1271–1276.
- Belov, A.V., Forbush Effects and Their Connection with Solar, Interplanetary and Geomagnetic Phenomena, *Proc. 25th of the Int. Astronomical Union*, Ioannina, 2009, Gopalswamy, N. and Webb, D.W, Eds., vol. 257, pp. 439–450.
- Belov, A., Eroshenko, E., Oleneva, V., Struminsky, A., and Yanke, V., What Determines the Magnitude of Forbush Decrease?, *Adv. Space Res.*, 2001, vol. 27, no. 3, pp. 625–630.
- Belov, A., Baisultanova, L., Eroshenko, E., Mavromichalaki, H., Yanke, V., Pchelkin, V., Plainaki, C., and Mariatos, G., Magnetospheric Effects in Cosmic Rays during the Unique Magnetic Storm on November 2003, *J. Geophys. Res.*, 2005a, vol. 110, p. A09S20; doi:10.1029/2005JA011067.
- Belov, A., Garcia, H., Kurt, V., Mavromichalaki, H., and Gerontidou, M., Proton Enhancements and Their Relation to X-Ray Flares during the Three Last Solar Cycles, *Sol. Phys.*, 2005b, vol. 229, no. 1, pp. 135–159.
- Burlaga, L., Berdichevsky, D., Gopalswamy, N., Lepping, R., and Zurbuchen, T., Merged Interaction Regions at 1 AU, *J. Geophys. Res.*, 2003, vol. 108, no. A12 SSH 2-1; doi: 10.1029/2003JA010088.
- Cane, H.V., Coronal Mass Ejections and Forbush Decreases, *Space Sci. Rev.*, 2000, vol. 93, nos. 1–2, pp. 55–77.
- Cane, H., Richardson, J., von Rosenvinge, T.T., and Wibberenz, G., Cosmic Ray Decreases and Shock Structure: A Multispacecraft Study, *J. Geophys. Res.*, 1994, vol. 99, pp. 21429–21441.
- Cane, H.V., Richardson, I.G., and von Rosenvinge, T.T., Cosmic Ray Decreases: 1964–1994, *J. Geophys. Res.*, 1996, vol. 101, pp. 21561–21572.
- Cliver, E.W. and Cane, H., The Angular Extents of Solar/Interplanetary Disturbances and Modulation of Galactic Cosmic Rays, *J. Geophys. Res.*, 1996, vol. 101, pp. 15533–15546.
- Crooker, N.U. and Cliver, E.W., Postmodern View of *M*-Regions, *J. Geophys. Res.*, 1994, vol. 99, pp. 23383–23388.
- Gonzalez, W.D., Tsuritani, B.T., McIntosh, P.S., and Clua De Gonzalez, A.L., Coronal Hole-Active Region-Cur-



- rent Sheet (CHARCS) Association with Intense Interplanetary and Geomagnetic Activity, *Geophys. Res. Lett.*, 1996, vol. 23, no. 19, pp. 2577–2581.
- Gopalswamy, N., Yashiro, S., Krucker, S., Stenborg, G., and Howard, R.A., Intensity Variation of Large Solar Energetic Particle Events Associated with Coronal Mass Ejections, *J. Geophys. Res.*, 2004, vol. 109, no. A12105.
- Haurwitz, M.W., Yoshida, S., and Akasofu, S.I., Interplanetary Magnetic Field Asymmetries and Their Effects on Polar Cap Absorption Events and Forbush Decreases, *J. Geophys. Res.*, 1965, vol. 70, pp. 2977–2988.
- Iucci, N., Parisi, M., Storini, M., and Villosi, G., Forbush Decreases: Origin and Development in the Interplanetary Space, *Nuovo Cimento*, 1979, vol. 2C, no. 4, pp. 1–52.
- Iucci, N., Parisi, M., Storini, M., Villosi, G., and Pinter, S., Longitudinal Dependence of the Interplanetary Perturbation Produced by Energetic Type 4 Solar Flares and of the Associated Cosmic Ray Modulation, *Proc. 19th ICRC*, San Diego, 1985, vol. 5, pp. 234–237.
- Iucci, N., Pinter, S., Parisi, M., Storini, M., and Villosi, G., The Longitudinal Asymmetry of the Interplanetary Perturbation Producing Forbush Decreases, *Nuovo Cimento*, 1986, vol. 9C, pp. 39–50.
- Richardson, I.G. and Cane, H.V., Signatures of Shock Drivers in the Solar Wind and Their Dependence on the Solar Source Location, *J. Geophys. Res.*, 1993, vol. 98, pp. 15295–15304.
- Sinno, K., Mechanism of Cosmic Ray Storms Inferred from Some Statistical Results, *Rep. Ionosph. Ionos. Space Res. Japan*, 1961, vol. 15, no. 2, pp. 276–279.